Fluid-dynamical scheme for equilibrium properties of two trapped fermion species with pairing interactions

P. Capuzzi,[1,2] E. S. Hernández,[1,2] and L. Szybisz[1,2,3]
[1]*Departamento de Física, Facultad de Ciencias Exactas y Naturales, Universidad de Buenos Aires, 1428 Buenos Aires, Argentina*
[2]*Consejo Nacional de Investigaciones Científicas y Técnicas, 1033 Buenos Aires, Argentina*
[3]*Departamento de Física, Comisión Nacional de Energía Atómica, 1428 Buenos Aires, Argentina*
(Received 25 June 2008; published 31 October 2008)

We present a generalization of the fluid-dynamical scheme developed for nuclear physics to the case of two trapped fermion species with pairing interactions. To establish a macroscopic description of the mass and momentum conservation laws, we adopt a generalization of the usual Thomas-Fermi approach that includes the pairing energy. We analyze the equilibrium density and gap profiles for an equal population mixture of harmonically trapped ^{6}Li atoms for different choices of the local equation of state. We examine slight departures from equilibrium within our formulation, finding that density oscillations can propagate as first sound coupled to pairing vibrations, that in a homogeneous fermion system exhibit a Bogoliubov-like quasiparticle spectrum. In this case, the dispersion relation for the coupled modes displays a rich scenario of stable, unstable, and damped regimes.

DOI: 10.1103/PhysRevA.78.043619 PACS number(s): 03.75.Ss, 05.30.Fk, 67.85.Lm

I. INTRODUCTION

Shortly after the first achievement of Fermi degeneracy in magnetically trapped ^{40}K atoms [1], followed by detection of superfluidity in optically confined ^{6}Li [2], resonant superfluidity [3] and pair condensation [4] across the crossover between a Bose-Einstein condensate (BEC) of tightly bound fermion dimers and a Bardeen-Cooper-Schrieffer (BCS) phase of weakly coupled fermion pairs crossover, the determination of the equation of state (EOS) of trapped Fermi species with pairing interactions drew the attention of many theorists. The use of mean-field theories can be traced back to the first application of the Thomas-Fermi (TF) theory to harmonically confined Fermi gases [5], valid when the Fermi energy ε_F is much greater than the trap spacing $\hbar\omega$; on these grounds, the local-density approximation (LDA) combined with the BCS theory for homogeneous systems became one of the most popular tools to investigate superfluidity in these systems [6], subject to specific limitations. In particular, the resource of replacing the chemical potential μ by the local shift $\mu - V(r)$ in the BCS expressions for particle densities and superfluid gap Δ is legitimate if the correlation length is much smaller than the harmonic oscillator length, and outside the small regions where either the local gap $\Delta(r)$ or $\varepsilon_F(r)$ vanishes. This means that the LDA can be used together with BCS in harmonic traps if the critical temperature T_c of the superfluid transition satisfies $\varepsilon_F \gg T_c \gg \hbar\omega$ [7]; consequently, it is not expected to hold at temperatures well below the superfluid transition where the Cooper pairs are large relative to the size of the trap. A recent derivation of the collective modes, starting from a quasiparticle transport equation [8,9], interpolates smoothly between superfluid hydrodynamics at zero temperature and the Vlasov equation at the critical one.

As a rule, the density and related quantities are weakly influenced by pairing correlations, since the latter involve a small fraction of particles around the Fermi level [10]. Moreover, little information about a normal-to-superfluid phase transition should be expected from e.g., examination of the low-energy collective frequencies [10,11]; among other alternatives, such as the calculation of the single-particle response of the gas to a modulation of the trap frequency [12], it has been proposed that the moment of inertia of the trapped cloud could reveal the onset of the BCS transition [13]. In fact, the rotational behavior of the trapped superfluid can be qualitatively different from that of a normal gas [14].

The combined schemes TF+BCS and TF+Hartree-Fock-Bogoliubov (HFB) have been extensively applied to atomic nuclei [15] (see, e.g., Refs. [13,16]). Reported mismatches [7] between TF+HFB and microscopic HFB calculations in a spherical harmonic trap at zero temperature have been improved [17] applying the regularization prescription in Ref. [18], finding good agreement for large particle numbers, roughly above 10^4. This adjustment can be drastically impaired as T_c is approached from below. More recently, it has been suggested that TF fits of experimental density profiles can in fact be applied to obtain information about the temperature T of the trapped system [19]. However, the validity of mean-field methods must be tested in the unitary regime [20] where the interacting particles are strongly correlated. As anticipated in Ref. [21], the EOS of a trapped system changes significantly across the BEC-BCS crossover, for which clear experimental evidence has been reported [22]. On the theoretical side, there is strong indication that a polytropic in the frame of standard superfluid hydrodynamics gives rise to a collective spectrum rather sensitive to the crossover [23], as confirmed by quantum Monte Carlo (QMC) calculations [24], and recent experiments [25].

In any method that resorts to the LDA, the TF prescription of the density of a trapped fermion species ignores any coupling to the anomalous pair density or to the gap. To the best of our knowledge, the presumption that this coupling is irrelevant throughout the whole range of applicability of the TF+BCS method has not been tested against any alternative mean-field treatment; within the dynamical schemes, standard superfluid hydrodynamics derives the time evolution of

the particle current from the chemical potential of the normal species (see, e.g., Ref. [23]), whose constant value in the equilibrium regime, determined by the number of particles, is the basis for the construction of the TF density. In this paper, we intend to take one step forward and explore further the effects of coupling between particle and anomalous densities. For this sake, we develop an extension of the fluid-dynamical (FD) scheme proposed for nuclear physics [26] in the 1970s as a macroscopic version of time-dependent Hartree-Fock theory (TDHF). In this spirit, stemming from a two-body Hamiltonian with pairing interactions, we construct a set of coupled equations of motion for the above densities and for the particle currents in coordinate representation, and propose a generalization of the TF description of normal fluids with a chemical potential that includes the contribution from the pairing energy. In the equilibrium regime, our equations are compatible with the BCS description of homogeneous systems; accordingly, we propose an alternative scheme to TF+BCS treatments in the presence of harmonic traps.

This paper is organized as follows. In Sec. II we establish our notation and shortly review the derivation of the Bogoliubov–de Gennes (BdG) equations [27–29] for asymmetric two fermion species. In Sec. III we present the FD description of paired fermions and in Sec. IV we analyze the equilibrium densities and gap, compared with TF+BCS and with quantum Monte Carlo (QMC) results, for different numbers of particles, and we analyze some global quantities as functions of the scattering length. Section V contains an analysis of small amplitude oscillations, focusing on a detailed examination of the coupled density and pairing vibrations in an homogeneous fermion system. The results and perspectives are summarized in Sec. VI.

II. GENERAL FORMALISM

The starting point for the formulation developed in Sec. III is a zero-temperature grand potential operator for two mutually interacting fermion species denoted as $\sigma=\pm$, with populations N_σ subject to external potentials $V_\sigma(\mathbf{r})$,

$$\begin{aligned}\hat{\Omega} &= H - \mu_+ N_+ - \mu_- N_- \\ &= \int d\mathbf{r} \sum_\sigma \left(-\frac{\hbar^2}{2m} \Psi_\sigma^\dagger(\mathbf{r}) \nabla^2 \Psi_\sigma(\mathbf{r}) \right. \\ &\quad \left. + [V_\sigma(\mathbf{r}) - \mu_\sigma] \Psi_\sigma^\dagger(\mathbf{r}) \Psi_\sigma(\mathbf{r}) \right) \\ &\quad + g \int d\mathbf{r} \Psi_+^\dagger(\mathbf{r}) \Psi_-^\dagger(\mathbf{r}) \Psi_-(\mathbf{r}) \Psi_+(\mathbf{r}). \end{aligned} \tag{2.1}$$

The basic dynamics of the field operators is contained in the equation of motion (EOM)

$$\begin{aligned}\imath\hbar \frac{\partial \Psi_\sigma(\mathbf{r})}{\partial t} &= \left(-\frac{\hbar^2}{2m} \nabla^2 + [V_\sigma(\mathbf{r}) - \mu_\sigma] \right. \\ &\quad \left. + g \Psi_{-\sigma}^\dagger(\mathbf{r}) \Psi_{-\sigma}(\mathbf{r}) \right) \Psi_\sigma(\mathbf{r}). \end{aligned} \tag{2.2}$$

The formalism is sufficiently general to make room to any lack of symmetry between species, including external potentials, unequal populations, and different propagation velocities $\mathbf{U}_\sigma = \hbar \mathbf{q}_\sigma / m$ of the field operators, generally expressed in terms of atomic operators $a_{\alpha\sigma}^\dagger$ and wave functions $\psi_{\alpha\sigma}(\mathbf{r})$ as

$$\Psi_\sigma(\mathbf{r}) = \sum_\alpha e^{\imath \mathbf{q}_\sigma \cdot \mathbf{r}} \psi_{\alpha\sigma}(\mathbf{r}) a_{\alpha\sigma}. \tag{2.3}$$

The one-body density and current operator for each fermion species are, respectively, defined as

$$\hat{\rho}_\sigma(\mathbf{r}, \mathbf{r}') = \Psi_\sigma^\dagger(\mathbf{r}') \Psi_\sigma(\mathbf{r}), \tag{2.4}$$

$$\hat{\mathbf{j}}_\sigma(\mathbf{r}, \mathbf{r}') = \frac{\hbar}{2m\imath} (\nabla - \nabla') \hat{\rho}_\sigma(\mathbf{r}, \mathbf{r}'), \tag{2.5}$$

and the pair operator representing the anomalous density is

$$\hat{\kappa}_\sigma(\mathbf{r}, \mathbf{r}') = \Psi_\sigma(\mathbf{r}) \Psi_{-\sigma}(\mathbf{r}') \equiv -\hat{\kappa}_{-\sigma}(\mathbf{r}', \mathbf{r}). \tag{2.6}$$

Introducing the one-body (particle-number conserving) mean-field Hamiltonian

$$H_\sigma(\mathbf{r}) = -\frac{\hbar^2}{2m} \nabla^2 + V_\sigma(\mathbf{r}) - \mu_\sigma + g \rho_{-\sigma}(\mathbf{r}) \tag{2.7}$$

and under Bogoliubov's transformation

$$\Psi_\sigma = \sum_\alpha (u_{\alpha\sigma} b_{\alpha\sigma} - v_{\alpha,-\sigma}^* b_{\alpha,-\sigma}^\dagger), \tag{2.8}$$

$$\Psi_{-\sigma}^\dagger = \sum_\alpha (u_{\alpha,-\sigma}^* b_{\alpha,-\sigma}^\dagger + v_{\alpha\sigma} b_{\alpha\sigma}) \tag{2.9}$$

with local functions $u_{\alpha\sigma}(\mathbf{r})$, $v_{\alpha\sigma}(\mathbf{r})$, the Bogoliubov–de Gennes (BdG) equations [27] read as

$$\imath\hbar \dot{u}_{\alpha\sigma} = H_\sigma u_{\alpha\sigma} + \Delta_\sigma v_{\alpha\sigma}, \tag{2.10}$$

$$\imath\hbar \dot{v}_{\alpha\sigma} = -H_{-\sigma} v_{\alpha\sigma} + \Delta_\sigma^* u_{\alpha\sigma} \tag{2.11}$$

with the gap matrix $\Delta_\sigma = -g\kappa_\sigma$. From Eq. (2.6), it is clear that the gap density is independent of σ, i.e., one has $|\Delta|^2 \equiv |\Delta_\sigma|^2 = |\Delta_{-\sigma}|^2$. Instead, in the stationary BCS regime with quasiparticle energies $E_{\alpha\sigma}$, both the normal and anomalous densities depend upon σ, at arbitrary temperature, through the Fermi occupation numbers $f_{\alpha\sigma} = \langle b_{\alpha\sigma}^\dagger b_{\alpha\sigma} \rangle = 1/(1 + e^{E_{\alpha\sigma}/T})$, since one has

$$\rho_\sigma(\mathbf{r}, \mathbf{r}') = \sum_\alpha [u_\alpha^*(\mathbf{r}) u_\alpha(\mathbf{r}') f_{\alpha\sigma} + v_\alpha(\mathbf{r}) v_\alpha^*(\mathbf{r}') (1 - f_{\alpha,-\sigma})], \tag{2.12}$$

$$\kappa_\sigma(\mathbf{r}, \mathbf{r}') = \sum_\alpha [u_\alpha(\mathbf{r}) v_\alpha^*(\mathbf{r}') (1 - f_{\alpha\sigma}) - v_\alpha^*(\mathbf{r}) u_\alpha(\mathbf{r}')\ f_{\alpha,-\sigma})]. \tag{2.13}$$

In the mean-field approximation, the expectation value $\Omega = \langle \hat{\Omega} \rangle$ of the grand potential operator (2.1) reads as

$$\Omega = \int d\mathbf{r}\left(\varepsilon - \sum_\sigma \mu_\sigma \rho_\sigma\right) = \int d\mathbf{r}\left(\sum_\sigma [\tau_\sigma + (V_\sigma - \mu_\sigma)\rho_\sigma] + g\rho_+\rho_- + \frac{|\Delta|^2}{g}\right), \tag{2.14}$$

where $\varepsilon(\mathbf{r})$ is the energy density kernel and $\tau_\sigma(\mathbf{r}) = \langle \Psi_\sigma^\dagger(\mathbf{r})(-\hbar^2\nabla^2/2m)\Psi_\sigma(\mathbf{r})\rangle$ is the kinetic energy density of species σ, whose chemical potential is given by

$$\mu_\sigma = \frac{\partial \varepsilon}{\partial \rho_\sigma} = \frac{\partial \tau_\sigma}{\partial \rho_\sigma} + V_\sigma + g\rho_{-\sigma} + \frac{1}{g}\frac{\partial |\Delta|^2}{\partial \rho_\sigma}. \tag{2.15}$$

Expressions for the diagonal matrix elements of the densities, kinetic energy density, currents, and other relevant formulas are collected in Appendix A. We also notice that when the field operators acquire velocities $\mathbf{U}_\sigma$, which amounts to endowing the amplitudes u_α, v_α^* with phase factors $e^{i\mathbf{q}_\sigma\cdot\mathbf{r}}$, the Hamiltonian H_σ simply switches to $H_\sigma + \hbar^2 q_\sigma^2/2m$.

III. FLUID-DYNAMICAL EQUATIONS OF MOTION

Nuclear FD [15,26] derived from the TDHF EOM for the single-particle density matrix is the collisionless version of hydrodynamics. The FD EOM's are formally identical to those of classical hydrodynamics and include kinetic energy terms that give rise to quantal pressure. Although it has been extended to include pairing interactions through the Wigner transform of the generalized density matrix [16], to the best of our knowledge, none of the previous treatments of pairing interactions within a quasiclassical scheme [30] have considered the coupling between particle and pair density induced by the presence of the pairing energy in the EOS. In this section, we generalize the previous formulation of FD [26] incorporating BCS theory for trapped ultracold fermions [7].

A. Densities

Using Eq. (2.2), it is straightforward to derive the mean-field EOM for the spatial matrix elements of the densities (2.4) of either fermion species,

$$\imath\hbar\frac{\partial}{\partial t}\rho_\sigma(\mathbf{r},\mathbf{r}') = [H_\sigma(\mathbf{r}) - H_\sigma(\mathbf{r}')]\rho_\sigma(\mathbf{r},\mathbf{r}') + g[\kappa_\sigma(\mathbf{r},\mathbf{r})\kappa_\sigma^*(\mathbf{r}',\mathbf{r}) - \kappa_\sigma^*(\mathbf{r}',\mathbf{r}')\kappa_\sigma(\mathbf{r},\mathbf{r}')]. \tag{3.1}$$

Is it convenient to introduce center-of-mass coordinates $(\mathbf{R},\mathbf{s})$ with $\mathbf{r}=\mathbf{R}+\mathbf{s}/2$ and $\mathbf{r}'=\mathbf{R}-\mathbf{s}/2$. One readily reaches the continuity equation for each diagonal one-body density

$$\frac{\partial}{\partial t}\rho_\sigma(\mathbf{r}) = -\boldsymbol{\nabla}\cdot\mathbf{j}_\sigma(\mathbf{r}). \tag{3.2}$$

Similarly, the EOM for the anomalous density can be expressed as

$$\imath\hbar\frac{\partial}{\partial t}\kappa_\sigma(\mathbf{r},\mathbf{r}') = [H_\sigma(\mathbf{r}) + H_{-\sigma}(\mathbf{r}')]\kappa_\sigma(\mathbf{r},\mathbf{r}') - g[\rho_{-\sigma}(\mathbf{r}',\mathbf{r})\kappa_\sigma(\mathbf{r},\mathbf{r}) + \rho_\sigma(\mathbf{r},\mathbf{r}')\kappa_\sigma(\mathbf{r}',\mathbf{r}')] + g\delta(\mathbf{s})\kappa_\sigma(\mathbf{r}',\mathbf{r}'). \tag{3.3}$$

Keeping in mind that the pairing tensor diverges for s approaching zero, we introduce the gap matrix and the regular part $\kappa_{\sigma\,\mathrm{reg}}$ of κ_σ according to [7]

$$\Delta_\sigma(\mathbf{R},\mathbf{s}) = -g\kappa_{\sigma\,\mathrm{reg}}(\mathbf{R},\mathbf{s}), \tag{3.4}$$

$$\kappa_\sigma(\mathbf{R},\mathbf{s}) = \frac{m}{4\pi\hbar^2}G_\mu(\mathbf{s})\Delta_\sigma(\mathbf{R}) + \kappa_{\sigma\,\mathrm{reg}}(\mathbf{R},\mathbf{s}) \tag{3.5}$$

with G_μ as the one-body Green's function satisfying the equation

$$(\nabla_\mathbf{s}^2 + k_\mu^2)G_\mu(\mathbf{s}) = -4\pi\delta(\mathbf{s}) \tag{3.6}$$

for $k_\mu^2 = m(\mu_{\mathrm{total}} - g\rho_{\mathrm{total}})/\hbar^2$, the subscript total indicating summation of the contributions from both species. After substitution of Eqs. (3.4) and (3.5) into (3.3), we find the EOM

$$\imath\hbar\frac{\partial}{\partial t}\kappa_{\sigma\,\mathrm{reg}}(\mathbf{r},\mathbf{r}') = [H_\sigma(\mathbf{r}) + H_{-\sigma}(\mathbf{r}')]\kappa_{\sigma\,\mathrm{reg}}(\mathbf{r},\mathbf{r}') + \rho_{-\sigma}(\mathbf{r}',\mathbf{r})\Delta_\sigma(\mathbf{r}) + \rho_\sigma(\mathbf{r},\mathbf{r}')\Delta_\sigma(\mathbf{r}'). \tag{3.7}$$

Accordingly, taking the limit of Eq. (3.7) as s approaches 0, in view of Eq. (3.4) we obtain for the diagonal anomalous density

$$\imath\hbar\frac{\partial}{\partial t}\kappa_{\sigma\,\mathrm{reg}}(\mathbf{r}) = \left(-\frac{\hbar^2}{4m}\nabla_\mathbf{r}^2 + V_{\mathrm{total}}(\mathbf{r}) - \mu_{\mathrm{total}}\right)\kappa_{\sigma\,\mathrm{reg}}(\mathbf{r}) + \lim_{s\to 0}\left(-\frac{\hbar^2}{m}\nabla_\mathbf{s}^2\kappa_{\sigma\,\mathrm{reg}}(\mathbf{r},\mathbf{s})\right). \tag{3.8}$$

In the uniform system with equal populations and in the absence of any external field, the equilibrium solution of Eq. (3.8) satisfies the identity

$$\lim_{s\to 0}\left(\frac{\hbar^2}{m}\nabla_\mathbf{s}^2\kappa_{\sigma\,\mathrm{reg}}(\mathbf{s})\right) = \frac{\Delta_\sigma^{(0)}\mu_{\mathrm{total}}^{(0)}}{g} \tag{3.9}$$

with $\mu_{\mathrm{total}}^{(0)} = \mu_+^{(0)} + \mu_-^{(0)}$ the chemical potential of a two species, homogeneous Fermi gas in the presence of their mutual interaction, and $\Delta_\sigma^{(0)}$ the corresponding gap. According to Eq. (2.15), each chemical potential is

$$\mu_\sigma^{(0)} = \frac{\partial \tau_\sigma^{(0)}}{\partial \rho_\sigma^{(0)}} + g\rho_{-\sigma}^{(0)} + \frac{1}{g}\frac{\partial |\Delta_\sigma^{(0)}|^2}{\partial \rho_\sigma^{(0)}}. \tag{3.10}$$

Thus, we propose an LDA frame where the gap satisfies the equation

$$\imath\hbar\frac{\partial \Delta_\sigma(\mathbf{r})}{\partial t} = \left(-\frac{\hbar^2}{4m}\nabla^2 + V_{\mathrm{total}}(\mathbf{r}) - \mu_{\mathrm{total}}\right)\Delta_\sigma(\mathbf{r}) + \mu_{\mathrm{total}}^{(0)}[\rho(\mathbf{r})]\Delta_\sigma^{(0)}[\rho(\mathbf{r})]. \tag{3.11}$$

B. Current

In the center-of-mass system, the current operator acting on densities is $\hbar/m\imath\nabla_{\mathbf{s}}$. The corresponding EOM for the spatial matrix elements of the current can be written from Eq. (3.1). However, for the local current $\mathbf{j}_\sigma(\mathbf{r})$ a shortcut is as follows: Being [cf. Eq. (2.5)]

$$\imath\hbar\frac{\partial}{\partial t}\mathbf{j}_\sigma = \frac{\hbar^2}{2m}\frac{\partial}{\partial t}\langle\Psi_\sigma^\dagger\nabla\Psi_\sigma - (\nabla\Psi_\sigma^\dagger)\Psi_\sigma\rangle \tag{3.12}$$

in a stationary state where the fields oscillate as $\Psi_\sigma(\mathbf{r},t) = \Psi_\sigma(\mathbf{r})e^{\imath E_\sigma t}$ the above equation acquires the standard hydrodynamical appearance

$$\frac{\partial}{\partial t}\mathbf{j}_\sigma = -\frac{\rho_\sigma}{m}\nabla E_\sigma. \tag{3.13}$$

Accordingly, the main hypothesis of this work is that the local quasienergy field $E_\sigma(\mathbf{r})$ satisfies the same relation as in a normal fluid, namely

$$E_\sigma(\mathbf{r}) = \frac{\partial\varepsilon}{\partial\rho_\sigma} \equiv \mu_\sigma(\mathbf{r}) \tag{3.14}$$

so that the current derives from the local chemical potential in the pairing field, as defined by Eq. (2.15).

The fluid-dynamical EOM's for the paired system are then the set of Eqs. (3.2), (3.11), and (3.13) together with (3.14). The equilibrium situation of the paired system is thus described by the coupled set

$$\nabla\mu_\sigma^{\mathrm{STF}} = 0, \tag{3.15}$$

$$\left(-\frac{\hbar^2}{4m}\nabla^2 + V_{\mathrm{total}} - \mu_{\mathrm{total}}\right)\Delta_\sigma^{\mathrm{FD}} + \mu_{\mathrm{total}}^{(0)}[\rho]\Delta_\sigma^{(0)}[\rho] = 0 \tag{3.16}$$

with real FD gap $\Delta_\sigma^{\mathrm{FD}}(\mathbf{r})$. These equations can be verified to hold in the homogeneous case, so Eq. (3.15) together with (2.15) defines the superfluid Thomas-Fermi (STF) particle density, which for vanishing gap reproduces the standard TF density of a normal Fermi gas. Although it may appear that STF is a straightforward generalization of TF, a major difference between this formalism and previous approaches is the substitution of the BCS gap equation by the local relation (3.16) that includes a quantum gap pressure by means of the kinetic operator.

IV. RESULTS AND DISCUSSION

We solve Eq. (3.15) for two fermion species trapped in a harmonic oscillator potential $V_\pm(\mathbf{r}) = m\omega^2 r^2/2$ within the LDA, by adopting several forms of the EOS and gap for homogeneous systems. We consider three specific approximations, namely, (i) the full solution for paired fermions with arbitrary coupling in the form calculated by Papenbrock and Bertsch [32] (PB) hereafter noted as STF+PB; (ii) the standard TF+BCS in the weak coupling limit, with EOS and gap,

$$\mu_\sigma^{\mathrm{TF}} = \frac{\hbar^2 k_F^2}{2m} + g\rho_{-\sigma}, \tag{4.1}$$

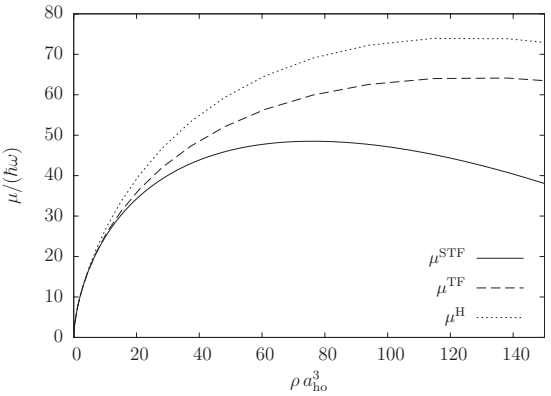

FIG. 1. Chemical potentials μ^H, μ^{TF}, and μ^{STF} in units of the oscillator energy (see text for details) as functions of dimensionless density for a homogeneous mixture of ^{6}Li atoms with $a = -114$ nm.

$$\Delta^{\mathrm{BCS}} = \frac{8}{e^2}\frac{\hbar^2 k_F^2}{2m}\exp\left(-\frac{\pi}{2k_F|a|}\right), \tag{4.2}$$

where $k_F = (6\pi^2\rho_\sigma)^{1/3}$ is the local Fermi momentum; (iii) the EOS and gap obtained from QMC calculations in Refs. [31,33,34] (STF+QMC). In Ref. [34] both the energy per particle and the gap have been computed along the BEC-BCS crossover through the unitary regime, with a fermion-fermion interaction described by a square-well potential, however short-ranged with respect to the mean interparticle distance.

In the original PB treatment, one finds through dimensional regularization of integrals (see Appendix B) that when $\rho_+ = \rho_- = \rho$ the kinetic energy density is given by

$$\tau_\sigma = -\frac{3}{10}\frac{k_{\mu\sigma}^3}{4\pi}\lambda(1+x_\sigma^2)^{3/4}\left[P_{3/2}\left(-\frac{1}{\sqrt{1+x_\sigma^2}}\right) + \sqrt{1+x_\sigma^2}P_{1/2}\left(-\frac{1}{\sqrt{1+x_\sigma^2}}\right)\right] \tag{4.3}$$

and the gap equation can be written as

$$\frac{1}{k_{\mu\sigma}a} = (1+x_\sigma^2)^{1/4}P_{1/2}\left(-\frac{1}{\sqrt{1+x_\sigma^2}}\right), \tag{4.4}$$

where $k_{\mu\sigma} = \sqrt{2m\lambda_\sigma/\hbar^2}$, $x_\sigma = \Delta_\sigma/\lambda_\sigma$, P_α are Legendre functions, and λ_σ is the shifted chemical potential $\lambda_\sigma = \mu_\sigma - g\rho_{-\sigma}$. To illustrate the main characteristics of this approach, we first consider a homogeneous system of ^{6}Li atoms with identical spin populations, so that the label σ can be suppressed hereafter. The species interact with a scattering length $a = -114$ nm [17] and we compute the common chemical potential $\mu^H = \partial\tau/\partial\rho + g\rho$ from the above equations. In Fig. 1 we show this chemical potential together with μ^{TF} from Eq. (4.1) (dotted and dashed lines, respectively), as functions of partial density times the cubed oscillator length a_{ho}. The full line represents μ^{STF} from Eq. (3.15). It is worth noting that all STF+PB expressions reduce to the TF+BCS ones at low densities, so that we may only expect differences for large numbers of particles. We verify that all curves present a

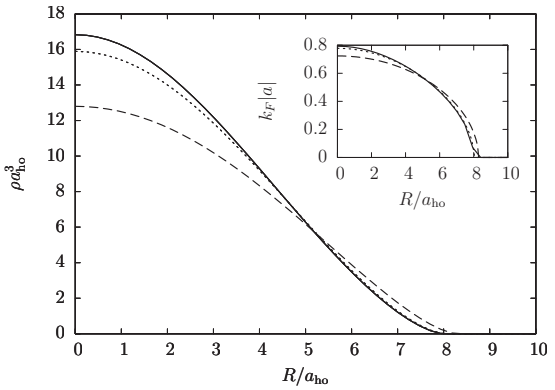

FIG. 2. Dimensionless density profiles for ^{6}Li atoms in a mixture with $N_\pm = 8.5\times 10^3$ and $a=-114$ nm in the STF+PB (solid lines), TF+BCS (dotted lines), and STF+QMC (dashed lines) approximations. The inset displays the local Fermi momentum k_F times $|a|$.

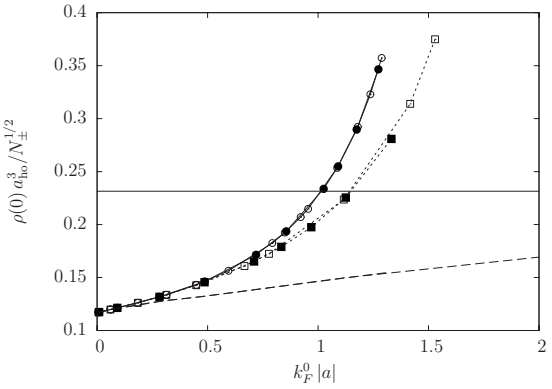

FIG. 3. Dimensionless particle densities $\rho(0)=(k_F^0)^3/6\pi^2$ at the trap center as functions of $k_F^0|a|$ for several EOS's and particle numbers. The solid, dotted, and dashed lines with symbols correspond to the STF, BCS, and QMC EOS, respectively. Empty symbols correspond to $N_\pm = 8500$ and full symbols to $N_\pm = 10^5$. The solid horizontal line indicates the value of $\rho(0)$ in the unitarity limit.

maximum, meaning that for larger densities, the system is thermodynamically unstable; this collapse is known to be an artifact at $T=0$ resulting from the use of mean-field EOS [6] and takes place at a lower density within the STF+PB frame. We note that predicted mechanical instability of a Fermi gas in the presence of attractive interactions [6] does not appear in actual experiments carried up to very high densities [35].

In Fig. 2 we show the density profiles evaluated using the three EOS's for a lithium mixture with $N_+ \equiv N_- = 8.5\times 10^3$ atoms. For the chosen interaction strength the particle densities predicted by these EOS's mainly differ at the trap center, where both the TF+BCS and STF+PB results are larger than the STF+QMC ones. On the other hand, the widths of the profiles are roughly the same for all EOS's. The increase of the density in the STF+PB calculation can be attributed to the contribution of the gap density to the EOS; as seen in Eq. (2.15), the term Δ_σ^2 provides an additional negative pressure which is stronger at larger densities, i.e., at the trap center. This effect accounts for the 6% difference of the central densities with respect to the TF+BCS prediction. For larger $|a|$ both the STF+PB and the TF+BCS EOS's predict a transition to a collapsed phase, as illustrated in Fig. 3 where the particle densities at the trap center are plotted as functions of the scattering length, including the limiting value of ρ predicted for infinite $|a|$ in the so-called unitarity limit [23], where the QMC approach provides a quantitatively correct EOS.

Once the particle densities and total chemical potential $\mu_{\rm total}$ are computed we numerically solve the nonlocal gap equation (3.16). For that matter, we cast the inhomogeneous differential equation into an algebraic system by expanding the FD gap profile in the three-dimensional harmonic oscillator basis with $l=0$ due to the spherical symmetry of the system, $\phi_i(\mathbf{r})$. The FD gap is thus written as

$$\Delta^{\rm FD}(\mathbf{r}) = \sum_i c_i \phi_i(\mathbf{r}), \tag{4.5}$$

where the coefficients c_i are straightforwardly calculated as

$$c_i = -\int \frac{\phi_i^*(\mathbf{r})\mu_{\rm total}^{(0)}[\rho]\Delta_\sigma^{(0)}[\rho]}{\epsilon_i - \mu_{\rm total}} d\mathbf{r} \tag{4.6}$$

with the oscillator energy for $l=0$, $\epsilon_i=(2i+3/2)\hbar\omega$. Furthermore, the spatial integrations were performed using a Gauss-Legendre quadrature with 3000 points and the infinite sum in (4.5) was truncated to $i=300$.

Figure 4 displays the spatial profiles of the gap obtained in this manner for the three EOS's, compared to $\Delta_\sigma(\mathbf{r})$ given by the local PB in Eq. (4.4) in terms of the STF density from Eq. (3.15), displayed with circles. We see that the Laplacian term induces oscillations in the gap profile around the trap center with wavelength comparable with the oscillator length, without modifying its spatial extent. This quantum gap pressure can be regarded as a perturbation for the TF+BCS gap equation (4.2), and by analyzing the ratio $\nabla^2\Delta^{(0)}[\rho]/\mu^{(0)}[\rho]$ one can see that this contribution decreases exponentially fast for ρ approaching zero, while it can be sizeable at the trap center for a large number of particles. This is consistent with our numerical findings reported in Fig. 4. For the largest particle number considered (bottom panel) we observe that the amplitude oscillations near the origin are flattened out.

To quantify the global dependence of the gap with the interaction we have evaluated the gap strength defined as

$$S = \int d\mathbf{r}\Delta(\mathbf{r}). \tag{4.7}$$

The results are shown in Fig. 5 and demonstrate that in addition to the usual $N^{1/2}$ scaling (cf. Fig. 2), TF+BCS overestimates the total strength at the crossover region. This may appear surprising at first sight since the TF+BCS gap profiles in Fig. 4 lie below the SFT+PB ones. However, one should keep in mind the presence of the r^2 Jacobian in the integral (4.7), in addition to the scaling of the horizontal axis in Fig. 5 by the central density.

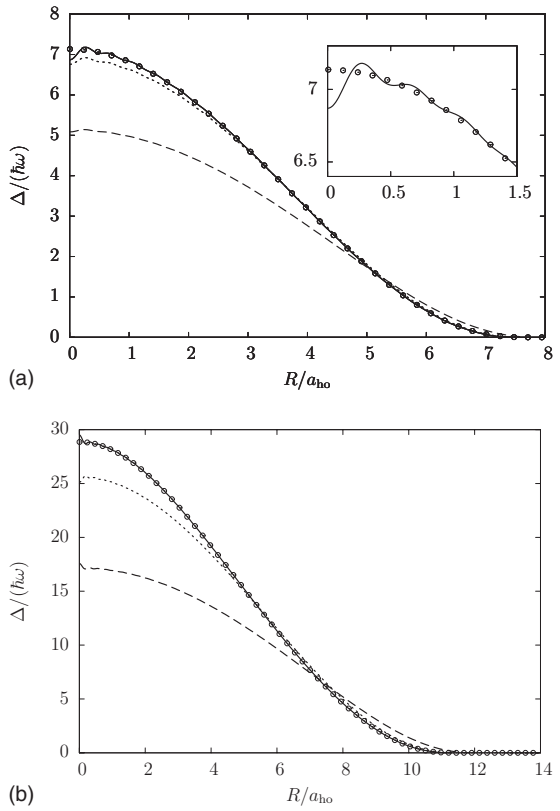

FIG. 4. Spatial gap profiles for $N_{\pm}=8500$ with $a=-114$ nm (top panel) and $N_{\pm}=10^5$ and $a=-90$ nm (bottom panel). Solid, dotted, and dashed lines correspond to the results of our STF+PB, TF+BCS, and STF+QMC EOS's, respectively. Empty circles denote the result for Eq. (4.4) with the STF density as an input.

V. SMALL AMPLITUDE OSCILLATIONS: FIRST SOUND AND PAIRING VIBRATIONS

Recently, the excitation spectrum of a Fermi gas in the crossover region has been tested both experimentally [25], revealing the pairing gap, and theoretically [24], indicating an important dependence of the results on the assumed fermionic EOS. In this section we restrict ourselves to two homogeneous fermion species and demonstrate that the current FD scheme may give rise to non-negligible coupling between first sound and pairing vibrations. We begin by noting that out of equilibrium the complex gap can be written as $\Delta_\sigma=|\Delta_\sigma|e^{i2m\Sigma_\sigma/\hbar}$, with Σ_σ the superfluid velocity potential, i.e., the superfluid velocity is $\mathbf{U}_S(\mathbf{r})=\nabla\Sigma_\sigma$. It is then natural to introduce the gap density $\rho_\Delta=|\Delta_\sigma|^2$. The set of FD equations can then be written as

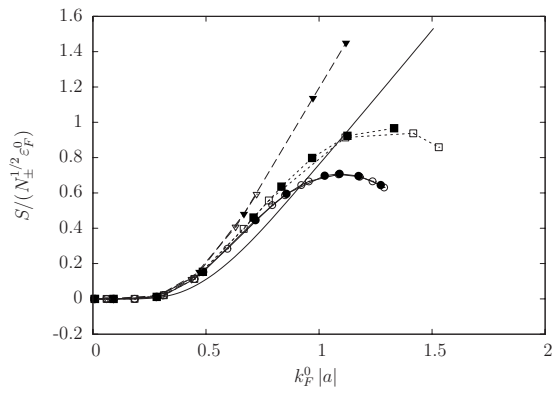

FIG. 5. Gap strengths S as functions of $k_F^0|a|$. The line styles are the same as in Fig. 3 and ε_F^0 indicates the local Fermi energy at the trap center.

$$\frac{\partial\rho_\sigma}{\partial t}=-\nabla\cdot(\rho_\sigma\mathbf{U}_\sigma), \tag{5.1}$$

$$\left(\frac{\partial}{\partial t}+\mathbf{U}_\sigma\cdot\nabla\right)\mathbf{U}_\sigma=-\frac{1}{m}\nabla\mu_\sigma, \tag{5.2}$$

$$\frac{\partial\rho_\Delta}{\partial t}=-\nabla\cdot(\rho_\Delta\mathbf{U}_S), \tag{5.3}$$

$$\frac{\partial}{\partial t}\mathbf{U}_S=-\frac{1}{2m}\nabla\Phi. \tag{5.4}$$

Here we have introduced the Bernoulli-like potential for the superfluid velocity [cf. Eq. (3.11)]

$$\Phi=\frac{1}{\Delta_\sigma^{\rm FD}}\left[\left(-\frac{\hbar^2}{4m}\nabla^2-\mu_{\rm total}\right)\Delta_\sigma^{\rm FD}+\mu_{\rm total}^{(0)}[\rho]\Delta_\sigma^{(0)}[\rho]\right] \tag{5.5}$$

that vanishes in equilibrium.

When the densities experience variations $\delta\rho_\sigma,\delta\rho_\Delta$ with respect to their equilibrium values ρ_σ and ρ_Δ, and the system sets into motion with small velocities $\mathbf{U}_\sigma$ and $\mathbf{U}_S$, the linearized EOM's for the fluctuations give rise to coupled wave propagation of first sound and pairing vibrations [37,38] of the form

$$\frac{\partial^2\delta\rho_\sigma}{\partial t^2}=\frac{\rho_\sigma}{m}\nabla^2\delta\mu_\sigma, \tag{5.6}$$

$$\frac{\partial^2\delta\rho_\Delta}{\partial t^2}=\frac{\rho_\Delta}{2m}\nabla^2\delta\Phi, \tag{5.7}$$

where in turn $\delta\Phi$ reads as

$$\delta\Phi=-\frac{\hbar^2}{8m}\frac{\nabla^2\delta\rho_\Delta}{\rho_\Delta}+\delta\mu_{\rm total}. \tag{5.8}$$

In the case of an homogeneous system with equal populations, where $\mu_+=\mu_-\equiv\mu$, a dispersion relation can be found analytically; assuming that all fluctuations propagate with a phase factor $e^{i(\mathbf{k}\cdot\mathbf{r}-\omega t)}$, we readily find the algebraic system (suppressing σ labels)

$$(\omega^2-c_\rho^2k^2)\delta\rho-\frac{\rho}{m}\left(\frac{\partial\mu}{\partial\rho_\Delta}\right)k^2\delta\rho_\Delta=0, \tag{5.9}$$

$$-\frac{\rho}{m}\left(\frac{\partial\mu}{\partial\rho}\right)k^2\delta\rho+\left(\omega^2-c_\Delta^2k^2-\frac{\hbar^2k^4}{16m^2}\right)\delta\rho_\Delta=0 \tag{5.10}$$

with the velocities

$$c_\rho^2 = \frac{\rho}{m}\left(\frac{\partial \mu}{\partial \rho}\right), \tag{5.11}$$

$$c_\Delta^2 = \frac{\rho_\Delta}{2m}\left(\frac{\partial \mu}{\partial \rho_\Delta}\right). \tag{5.12}$$

We observe that the pure modes, density first sound and pairing vibrations, propagate with frequencies

$$\omega_\rho = c_\rho k, \tag{5.13}$$

$$\omega_\Delta = \sqrt{c_\Delta^2 k^2 + \frac{\hbar^2 k^4}{16m^2}}. \tag{5.14}$$

The latter Eq. (5.14) coincides with the dispersion relation within Bogoliubov's model for liquid ^{4}He [36], where perturbations with low momentum propagate as phonons with the velocity c_Δ, while for high wave vector the pairing excitations consist just of single pairs with frequency $\hbar k^2/(4m)$ (see also Ref. [34]). These pure modes cross at a momentum $k_{\rm cross}=4m(c_\rho^2-c_\Delta^2)/\hbar$, if existing. We note as well that while normal first sound is unstable for negative c_ρ^2, stable pairing vibrations appear for momenta larger than $k_\Delta=4m|c_\Delta|/\hbar$ even if $c_\Delta^2 \leqslant 0$.

In the STF frame, the chemical potential depends on the gap, thus the pairing velocity (5.12) is nonvanishing and the solution of Eq. (5.10) gives

$$\omega_\pm^2 = \frac{\omega_\rho^2+\omega_\Delta^2}{2} \pm \sqrt{\left(\frac{\omega_\rho^2+\omega_\Delta^2}{2}\right)^2 - \omega_\rho^2 \frac{\hbar^2 k^4}{16m^2}}. \tag{5.15}$$

From this dispersion relation, we realize that the modes decouple at high momentum and behave like pure density and pairing modes, while at low momentum, a spurious state associated to an overall translation of the system appears at $\omega=0$ and a coupled wave propagates with $|\omega| \simeq \sqrt{\omega_\rho^2+\omega_\Delta^2}$. One can wonder about the stability of these modes; the conditions under which $\omega_\pm^2$ is a positive quantity can be analytically worked out and are illustrated in Fig. 6, where we plot the frequencies of the pure and coupled modes as functions of the wave vector, for arbitrary combinations of signs and magnitudes of c_ρ^2 and c_Δ^2 selected for illustration purposes. All quantities are expressed in arbitrary units, which correspond to the choice $\hbar=m=1$ in this model calculation.

The description of the panels with the particular choices for the velocities are as follows: (a) $c_\rho^2=1$, $c_\Delta^2=0.5$. All modes are stable; the pure modes cross and the coupled oscillations repel each other, with ω_+ and ω_- asymptotically approaching ω_Δ and ω_ρ, respectively. In this case we observe a significant reduction of the ω_- frequency with respect to its asymptotic limit, the free first sound mode; (b) $c_\rho^2=-1$, $c_\Delta^2=0.5$. Although both first sound and the soundlike coupled mode ω_- are unstable, it is worth recalling that mechanical instability does not prevent the BCS-type pairing [20], and we appreciate the existence of stable gap fluctuations in this regime; (c) $c_\rho^2=-1$, $c_\Delta^2=-0.5$. First sound and the soundlike coupled mode are unstable, as well as the pure pairing mode below k_Δ, while the pairinglike coupled mode exists for all wave vectors. (d) $c_\rho^2=0.5$, $c_\Delta^2=1$. The pure modes repel each other like the coupled counterparts. (e) $c_\rho^2=-0.5$, $c_\Delta^2=1$ display essentially the same behavior as in panel (b) with different scaling and (f) $c_\rho^2=-0.5$, $c_\Delta^2=-1$ is also similar to panel (c).

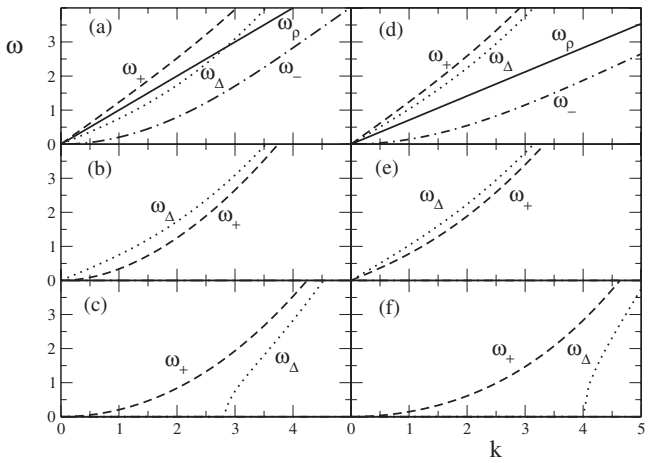

FIG. 6. Frequencies of the coupled modes together with those of pure first sound and pairing vibrations as functions of the wave vector, in an homogeneous fermion system with $\hbar=m=1$. The magnitudes are displayed in arbitrary units and the parameters in each panel are described in the text. As a guide, full, dotted, dashed, and dashed-dotted lines, respectively, correspond to first sound, pure pairing vibrations, and to the plus and minus coupled oscillations.

Another aspect of interest is the possible occurrence of damped modes, when the argument under the square root sign in Eq. (5.15) is negative. One can show that this can happen only for positive c_ρ^2 and negative c_Δ^2 and within a range of momenta $k_1 \leqslant k \leqslant k_2$, with $k_{1,2}=4m(c_\rho \pm |c_\Delta|)/\hbar$. This is depicted in Fig. 7 according to the description (a) $c_\rho^2=1$, $c_\Delta^2=-0.5$. It is clear that stable coupled modes exist for $k \leqslant k_1$ and $k \geqslant k_2$. The long-dashed line extending between these momenta is the common real part of the frequency $\omega_\pm$. (b) $c_\rho^2=0.5$, $c_\Delta^2=-1$. In this case, the pure pairing mode is unstable below k_Δ and k_1 is negative; thus, no stable, undamped coupled modes exist below k_2.

VI. SUMMARY

In this work we have extended fermion FD originally derived in nuclear physics to the case of trapped fermions with pairing interactions. We have obtained a set of coupled EOM's for the two particle densities and currents and for the newly defined FD gap. For an homogeneous system, the latter reduces to the well-known BCS gap equation. A similar

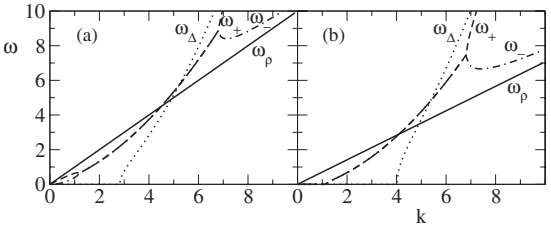

FIG. 7. Same as Fig. 6 for (a) $c_\rho^2=1$, $c_\Delta^2=-0.5$ and (b) $c_\rho^2=0.5$, $c_\Delta^2=-1$ (in arbitrary units).

EOM for the off-diagonal anomalous pair density was presented in Ref. [16] in relation to nuclear systems; however, these authors' derive a different continuity equation for the gap density. We note that the FD EOM's can be derived as well from the mean-field BdG equations in Sec. II As a main working hypothesis, in order to establish a macroscopic description of the mass and momentum conservation EOM's, we adopt a generalization of the usual TF approach that includes the pairing energy. To illustrate our proposal, we have analyzed the equilibrium density and gap profiles for an equal population mixture of harmonically trapped ^{6}Li atoms, by solving our static EOM's in the LDA spirit, according to different choices of the local EOS.

Our calculation can be classified as follows. On the one hand, we solve for the STF particle density using (a) the EOS obtained using the PB analytical formulas and (b) the EOS from QMC calculations existing in the literature. These two EOS yield the energy density as a function of both the particle densities and the gap. The particle density thus obtained is introduced as an input to obtain the FD gap. On the other hand, we solve the standard TF+BCS local equations. Although for sufficiently low densities the procedures STF +PB and TF+BCS give undistinguishable results, in good agreement with the STF+QMC ones, the effects of the gap density on the particle density, disregarded in the TF frame, are important at the trap center especially for moderate particle numbers. Moreover, the presence of the quantum gap pressure in the FD scheme is responsible for Friedel-like oscillations of the gap profile. This observation opens the possibility of investigating the FD gap in ^{3}He droplets up to a few thousand particles; however, since the pairing interaction acts in the spin-triplet channel and cannot be trivially represented by a contact interaction, the FD treatment is much more elaborated than the present one and calls for a separate line of research.

Finally, we have examined slight departures from equilibrium within our FD EOM's, finding that density oscillations can propagate as first sound coupled to pairing vibrations. The latter have been widely investigated in nuclear physics since the 1960s and are acknowledged to be one of the more important modes of collective motion in atomic nuclei; in the present case, we show that if the coupling to the particle density fluctuations can be neglected, the small amplitude pairing vibrations in a homogeneous fermion system exhibit a Bogoliubov-type quasiparticle spectrum similar to that in homogeneous ^{4}He. Moreover, for a translationally invariant fluid the dispersion relation for the coupled modes can be worked out analytically and displays a rich scenario of stable, unstable, and damped regimes, according to the possible values of the squared velocities of the pure modes. These scenarios are auspicious and encourage a separate investigation of this dynamics, as well as of large amplitude motion, in the case of inhomogeneous trapped systems, which will be the subject of a future work.

ACKNOWLEDGMENTS

This work was performed under Grant No. PICT 31980/05 from Agencia Nacional de Promoción Científica y Tecnológica, Grant No. PIP 5138/05 from Consejo Nacional de Investigaciones Científicas y Técnicas, and Grant No. X298 from Universidad de Buenos Aires, Argentina.

APPENDIX A

Here we collect the set of microscopic expressions for quantities appearing in the FD equations.

Bogoliubov amplitudes,

$$u_\alpha(\mathbf{r}) = |u_\alpha(\mathbf{r})|e^{\imath m/\hbar S_\alpha(\mathbf{r})}, \tag{A1}$$

$$v_\alpha^*(\mathbf{r}) = |v_\alpha(\mathbf{r})|e^{\imath m/\hbar S_\alpha(\mathbf{r})}. \tag{A2}$$

Particle velocity,

$$\mathbf{U}_\alpha(\mathbf{r}) = \nabla S_\alpha(\mathbf{r}). \tag{A3}$$

Particle density,

$$\rho_\sigma(\mathbf{r}) = \sum_\alpha [|u_\alpha(\mathbf{r})|^2 f_{\alpha\sigma} + |v_\alpha(\mathbf{r})|^2(1 - f_{\alpha,-\sigma})]. \tag{A4}$$

Particle kinetic energy,

$$\tau_\sigma(\mathbf{r}) = -\frac{\hbar^2}{2m}\sum_\alpha [|\nabla u_\alpha(\mathbf{r})|^2 f_{\alpha\sigma} + |\nabla v_\alpha(\mathbf{r})|^2(1 - f_{\alpha,-\sigma})]. \tag{A5}$$

Particle current,

$$\mathbf{j}_\sigma(\mathbf{r}) = \sum_\alpha [|u_\alpha(\mathbf{r})|^2 f_{\alpha\sigma} + |v_\alpha(\mathbf{r})|^2(1 - f_{\alpha,-\sigma})]\mathbf{U}_\alpha(\mathbf{r}). \tag{A6}$$

Anomalous density,

$$\kappa_\sigma(\mathbf{r}) = \sum_\alpha u_\alpha(\mathbf{r}) v_\alpha^*(\mathbf{r})(1 - f_{\alpha\sigma} - f_{\alpha,-\sigma}). \tag{A7}$$

APPENDIX B

In this section we compute integrals for the homogeneous system employing the regularization method developed in Ref. [32] (hereafter denoted as PB), where one uses energy integrals of the dimensionless form

$$\int_0^\infty \frac{z^\alpha}{\sqrt{(z-1)^2 + x^2}} = -\frac{\pi}{\sin \alpha\pi}(1 + x^2)^{\alpha/2} P_\alpha\left(-\frac{1}{\sqrt{1 + x^2}}\right). \tag{B1}$$

Here P_α is an associated Legendre function, $z = \epsilon/(\mu_\sigma - g\rho_{-\sigma})$, with ϵ the single-particle energy and $x_\sigma = \Delta/(\mu_\sigma - g\rho_{-\sigma})$. In terms of the Fermi momentum $k_{\mu\sigma} = \sqrt{2m(\mu_\sigma - g\rho_{-\sigma})/\hbar^2}$, given the single-particle density of states $\nu(\epsilon) = (2m^3)^{1/2}\epsilon^{1/2}/(2\pi^2)$ for each species, we can write

$$\nu(\epsilon)d\epsilon \equiv \nu_\sigma(z)dz = \frac{k_{\mu\sigma}^3}{4\pi^2} z^{1/2} dz. \tag{B2}$$

In this way we readily compute the following:

(1) The gap equation. The PB method computes the regular part of the anomalous density as the integral

$$\kappa_{\sigma\,\mathrm{reg}} = \frac{|\Delta_\sigma|}{2}\int_0^\infty \frac{\nu(\epsilon)d\epsilon}{\sqrt{(\epsilon-\mu_\sigma-g\rho_{-\sigma})^2+\Delta_\sigma^2}}, \tag{B3}$$

for any nonvanishing value of the gap $\Delta_\sigma=-g\kappa_{\sigma\,\mathrm{reg}}$ we obtain

$$\frac{1}{k_{\mu\sigma}a} = (1+x_\sigma^2)^{1/4}P_{1/2}\left(-\frac{1}{\sqrt{1+x_\sigma^2}}\right). \tag{B4}$$

(2) Particle density, being

$$\rho_\sigma = \int_0^\infty \nu(\epsilon)d\epsilon v_\sigma^2(\epsilon) \tag{B5}$$

the PB method gives

$$\begin{aligned}\rho_\sigma &= -\frac{1}{2}\int_0^\infty \nu_\sigma(z)dz\frac{z-1}{\sqrt{(z-1)^2+x_\sigma^2}}\\ &= -\frac{1}{2}\frac{k_{\mu\sigma}^3}{4\pi}(1+x_\sigma^2)^{1/4}\left[\sqrt{1+x_\sigma^2}P_{3/2}\left(-\frac{1}{\sqrt{1+x_\sigma^2}}\right)\right.\\ &\left. + P_{1/2}\left(-\frac{1}{\sqrt{1+x_\sigma^2}}\right)\right].\end{aligned} \tag{B6}$$

(3) Kinetic energy density,

$$\tau_\sigma = \int_0^\infty \epsilon\nu(\epsilon)d\epsilon v_\sigma^2(\varepsilon) \tag{B7}$$

gives, upon PB integration,

$$\begin{aligned}\tau_\sigma = \frac{1}{2}\frac{k_{\mu\sigma}^3}{4\pi}(\mu_\sigma-g\rho_{-\sigma})&\left[(1+x_\sigma^2)^{5/4}P_{5/2}\left(-\frac{1}{\sqrt{1+x_\sigma^2}}\right)\right.\\ &\left.+(1+x_\sigma^2)^{3/4}P_{3/2}\left(-\frac{1}{\sqrt{1+x_\sigma^2}}\right)\right].\end{aligned} \tag{B8}$$

Using the recurrence relation for associated Legendre functions with the current arguments, one has

$$P_{5/2} = -\frac{8}{5}\frac{P_{3/2}}{\sqrt{1+x_\sigma^2}} - \frac{3}{5}P_{1/2} \tag{B9}$$

according to which

$$\begin{aligned}\tau_\sigma = -\frac{3}{10}\frac{k_{\mu\sigma}^3}{4\pi}(\mu_\sigma-g\rho_\sigma)(1+x_\sigma^2)^{3/4}&\left[P_{3/2}\left(-\frac{1}{\sqrt{1+x_\sigma^2}}\right)\right.\\ &\left.+\sqrt{1+x_\sigma^2}P_{1/2}\left(-\frac{1}{\sqrt{1+x_\sigma^2}}\right)\right].\end{aligned} \tag{B10}$$

(4) Inhomogeneity in the gap equation: From Eq. (B3), we find

$$-\frac{\hbar^2}{m}\lim_{s\to 0}\nabla_{\mathbf{s}}^2\kappa_{\sigma\,\mathrm{reg}} = |\Delta_\sigma|\frac{k_{\mu\sigma}^3}{4\pi^2}\int_0^\infty \frac{z^{3/2}dz}{\sqrt{(z-1)^2+x_\sigma^2}} \tag{B11}$$

which gives

$$-\frac{\hbar^2}{m}\lim_{s\to 0}\nabla_{\mathbf{s}}^2\kappa_{\sigma\,\mathrm{reg}} = |\Delta_\sigma|\frac{k_{\mu\sigma}^3}{4\pi}(1+x_\sigma^2)^{3/4}P_{3/2}\left(-\frac{1}{\sqrt{1+x_\sigma^2}}\right). \tag{B12}$$

We can further verify that for the unpolarized configuration with $\rho_\sigma=\rho_{-\sigma}$, Eqs. (4.4), (B6), and (B12) reproduce Eq. (3.9).

[1] B. DeMarco and D. S. Jin, Science **285**, 1703 (1999).
[2] K. M. O'Hara, S. L. Hemmer, M. E. Gehm, S. R. Granade, M. E. Gehm, and J. E. Thomas, Science **298**, 2179 (2002).
[3] C. A. Regal and D. S. Jin, Phys. Rev. Lett. **90**, 230404 (2003).
[4] M. W. Zwierlein, C. A. Stan, C. H. Schunck, S. M. F. Raupach, A. J. Kerman, and W. Ketterle, Phys. Rev. Lett. **92**, 120403 (2004).
[5] D. A. Butts and D. S. Rokhsar, Phys. Rev. A **55**, 4346 (1997).
[6] M. Houbiers, R. Ferwerda, H. T. C. Stoof, W. I. McAlexander, C. A. Sackett, and R. G. Hulet, Phys. Rev. A **56**, 4864 (1997).
[7] G. Bruun, Y. Castin, R. Dum, and K. Burnett, Eur. Phys. J. D **7**, 433 (1999).
[8] M. Urban and P. Schuck, Phys. Rev. A **73**, 013621 (2006).
[9] M. Urban, Phys. Rev. A **75**, 053607 (2007).
[10] M. A. Baranov and D. S. Petrov, Phys. Rev. A **58**, R801 (1998).
[11] M. Urban and P. Schuck, Phys. Rev. A **67**, 033611 (2003).
[12] G. M. Bruun and C. W. Clark, J. Phys. B **33**, 3953 (2000).
[13] M. Farine, P. Schuck, and X. Viñas, Phys. Rev. A **62**, 013608 (2000).
[14] M. Cozzini and S. Stringari, Phys. Rev. Lett. **91**, 070401 (2003).
[15] P. Ring and P. Schuck, *The Nuclear Many Body Problem* (Springer, Berlin, 1980).
[16] M. Di Toro and V. M. Kolomietz, Z. Phys. A **328**, 285 (1987).
[17] M. Grasso and M. Urban, Phys. Rev. A **68**, 033610 (2003).
[18] A. Bulgac and Y. Yu, Phys. Rev. Lett. **88**, 042504 (2002).
[19] J. Stajic, Q. Chen, and K. Levin, Phys. Rev. Lett. **94**, 060401 (2005).
[20] H. Heiselberg, Phys. Rev. A **63**, 043606 (2001).
[21] J. R. Engelbrecht, M. Randeria, and C. A. R. Sá de Melo, Phys. Rev. B **55**, 15153 (1997).
[22] M. Greiner, C. A. Regal, and D. S. Jin, Nature (London) **426**, 537 (2003).
[23] H. Heiselberg, Phys. Rev. Lett. **93**, 040402 (2004).
[24] G. E. Astrakharchik, R. Combescot, X. Leyronas, and S. Stringari, Phys. Rev. Lett. **95**, 030404 (2005).
[25] M. Greiner, C. A. Regal, and D. S. Jin, Phys. Rev. Lett. **94**, 070403 (2005).
[26] C. Y. Wong, J. A. Maruhn, and T. A. Welton, Nucl. Phys. A **253**, 469 (1975).
[27] P. G. de Gennes, *Superconductivity of Metals and Alloys* (Benjamin, New York, 1966).
[28] J. F. Annett, *Superconductivity, Superfluids and Condensates*

(Oxford University Press, New York, 2004).
[29] A. J. Leggett, *Quantum Liquids: Bose Condensation and Cooper Pairing in Condensed-Matter Systems* (Oxford University Press, New York, 2006).
[30] J. W. Serene and D. Rainer, Phys. Rep. **101**, 221 (1983).
[31] G. E. Astrakharchik, J. Boronat, J. Casulleras, and S. Giorgini, Phys. Rev. Lett. **95**, 230405 (2005).
[32] T. Papenbrock and G. F. Bertsch, Phys. Rev. C **59**, 2052 (1999).
[33] J. Carlson, S. Y. Chang, V. R. Pandharipande, and K. E. Schmidt, Phys. Rev. Lett. **91**, 050401 (2003).
[34] G. E. Astrakharchik, J. Boronat, J. Casulleras, and S. Giorgini, Phys. Rev. Lett. **93**, 200404 (2004).
[35] M. E. Gehm, S. L. Hemmer, S. R. Granade, K. M. O'Hara, and J. E. Thomas, Phys. Rev. A **68**, 011401(R) (2003).
[36] P. Nozières and D. Pines, *The Theory of Quantum Liquids* (Addison-Wesley, New York, 1990).
[37] D. R. Bès and R. A. Broglia, Nucl. Phys. **80**, 289 (1966).
[38] A. Bohr and B. R. Mottelson, *Nuclear Structure* (Benjamin, Reading, MA, 1975).